Primary and Post-Surcharge Secondary Settlements of a Highway Embankment Constructed over Highly Organic Soils: A Case History

Liang Chern Chow, P.E., M.ASCE[1]; Joseph G. Bentler, P.E., M.ASCE[2]; and Richard A. Lamb, P.E., M.ASCE[3]

[1]American Engineering Testing, Inc., St. Paul, MN. E-mail: lchow@amengtest.com
[2]American Engineering Testing, Inc., St. Paul, MN. E-mail: jbentler@amengtest.com
[3]Minnesota Dept. of Transportation, Maplewood, MN. E-mail: rich.lamb@state.mn.us

ABSTRACT

A new segment of U.S. Highway 14 was constructed over highly organic clay near Nicollet, Minnesota, by using prefabricated vertical drains and surcharging in 2016. The highly compressible soils were predicted to settle 3 feet at the maximum fill area over the duration of 2 to 3 years. During the design phase, coefficient of consolidation (c_v) values obtained from 1-D consolidation tests were used to estimate the time-rate of settlement curve. The estimated primary settlement (S_p) of the embankment was about 37 inches after 6 months of surcharging. Nonetheless, a back-analysis using permeability change index (C_k), which has the advantage of representing decrease in permeability due to decrease in void ratio, was performed to model the primary settlement response of the highly organic soils. The computed settlement and pore water pressure show a good agreement with the field data. After the removal of surcharge, the post-surcharge settlement behavior, including rebound and compression, were continuously measured and recorded for more than a year. By using laboratory secondary compression index (C_α) and post-surcharge secondary compression indices (C'_α and C''_α) derived from the field data, the projection of embankment performance over the pavement design life was made.

INTRODUCTION

In the fall of 2016, Minnesota Department of Transportation (MnDOT) constructed a new segment of Westbound U.S. Highway 14 near Nicollet, MN as part of the Corridors of Commerce improvement project. In particular, an 800-foot stretch of the new segment would be constructed over swamplands containing highly organic silty clay loam. A total of twenty-five Cone Penetration Test (CPT) soundings (piezocones) and one Standard Penetration Test (SPT) boring that included thin-walled sampling were performed at the site for subsurface characterization. Overall, the investigation found a 34-ft thick layer of soft to very soft organic soil (swamp deposits) underlain by inorganic stiff glacial till with some sand seams. As presented in Figure 1, nearby CPT soundings clearly indicate highly organic soils to have tip stresses below 100 psi and friction ratios above 4%, whereas silty soils had tip stresses ranging from 100 to 350 psi and friction ratios of less than 3%. The Soil Behavior Type for the CPT soundings was determined to be 2 or 3 (organic soils or clay-silty clay) using the friction ratio (R_f) correlation proposed by Robertson et al. (1986). Groundwater was measured approximately 8 ft below the surface in the SPT boring at time of drilling.

During the design phase, a time-settlement assessment was made by using traditional one-dimensional consolidation theory and consolidation test data. The settlement predictions were as much as 30 to 37 inches of primary settlement followed by 3 to 6 inches of secondary settlement for the area of maximum fill over the design life of the pavement. Of particular concern, primary settlement was anticipated to occur during a period of 2 to 3 years (t_{90}) with the secondary compression continuing over several decades. Therefore, several ground improvement options were considered to mitigate the large settlement within a limited timeframe. The preferred option, consisting of prefabricated vertical drains (PVD), surcharging, and extended waiting periods, was selected as a good balance of cost and acceptable risk. In order to monitor embankment performance and further reduce geotechnical risk, MnDOT Geotechnical Section also developed a field instrumentation plan consisting of a MEMS-based horizontal "inclinometer" (ShapeAccelArray or SAA) and two nests of vibrating wire piezometers. The sensors were connected to an automated data collection system with near real-time online data hosting, which provided hourly measurements during both construction and post-construction periods.

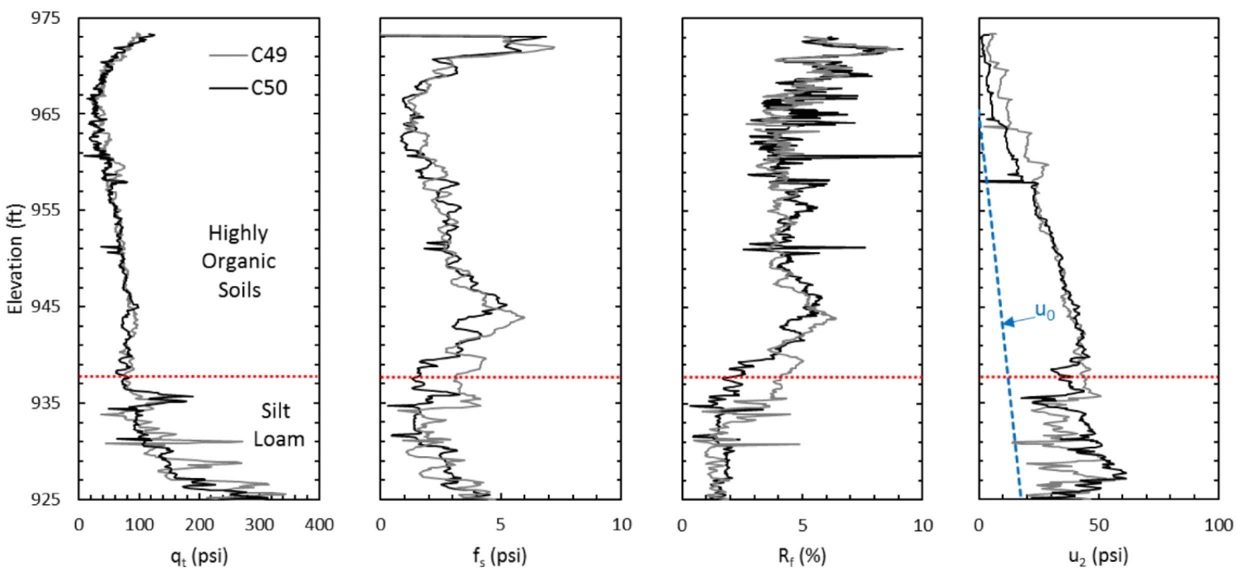

Figure 1. Nearby CPT soundings in area of thickest swamp deposits.

Soil behavior with respect to primary compression and excess pore water pressure were back-analyzed by using the computer program ILLICON (Mesri and Choi, 1985), starting from the first loading until the removal of surcharge. After that, rebound followed by secondary compression was evaluated to project the embankment performance over the next 25 years. The following sections discuss the development and characterization of subsurface profiles and parameters used for the analyses. Background details, including ground improvement options, design, and instrumentation details of the project can be found in Lamb et al. (2018).

SUBSURFACE CHARACTERIZATION

Moisture content, initial void ratio (e_0), and consolidation parameters

Example CPT soundings shown in Figure 1 provide a clear contrast of data between the very soft organic soil and relatively stiff silty soil. By using supplemental soil boring samples, the upper stratum was classified as organic to highly organic slightly plastic silt loam according to the MnDOT Textural Triangle classification. Unfortunately, Atterberg Limits data was not available to use for Unified Soil Classification System (USCS). Therefore, the USCS soil type based on MnDOT classification roughly corresponds to OL (organic silt) to MH (elastic silt). The underlying inorganic material was described as slightly plastic silt loam and sandy clay loam (MH to CL). The highly organic silt loam was found to have organic contents ranging from 7 to

32%, moisture contents of 71 to 166% and total unit weights ranging from 78 to 93 pcf. All of the moisture and organic contents from jar samples collected by MnDOT are presented in Figure 2(a). Initial void ratio e_0 was determined based on moisture content (MC), organic content (OC), and specific gravity by assuming a fully saturated profile, shown in Figure 2(b).

Table 1. The consolidation test results.

Depth (ft)	USCS Soil Type	MC (%)	e_0	P'_c (psf)	OCR	$C_{c\varepsilon}$*	C_r/C_c	c_v** (ft^2/day)
5.0	OL to MH	97	2.70	1,719	5.5	0.28	0.14	0.29
29.7	OL to MH	184	5.21	3,998	4.8	0.63	0.10	0.21
50.2	MH to CL	23	0.64	1,671	1.0	0.03	0.21	0.30

* $C_{c\varepsilon} = C_c/(1+e_0)$
** Estimated based on final vertical effective stress under maximum surcharge load, P'_{vs}.

In addition, three one-dimensional consolidation tests were performed on thin-walled tube samples within the organic and inorganic layers to determine the consolidation parameters shown in Table 1. These tests revealed that the organic soil was highly compressible and would consolidate significantly (3 to 10% axial strain) when loaded. As a check for sample disturbance, the retrieved samples had specimen quality designations (SQD) of B to C, indicating that sample disturbance was low to moderate. Based on the consolidation test results, the C_r values were 0.14, 0.4, and 0.01 for the top, middle, and bottom samples, respectively. The values of C_c derived within two times the preconsolidation pressure, P'_c range were 1.0 and 3.9, resulting in modified compression index, $C_{c\varepsilon}$ of 0.28 and 0.63 for the organic soils; the ratios of C_r/C_c are also reported in Table 1. As a reference, typical $C_{c\varepsilon}$ value is near 0.5 for soft clay and C_r/C_c ranges from 0.02 to 0.2 for most low to medium compressibility soils. The C_α/C_c value of 0.051 obtained from both top and middle samples agrees with typical values for organic clays and silts (Terzaghi et al. 1996).

Effective vertical stress (P'_v) and preconsolidation pressure (P'_c)

Based on the MC, e_0 and P'_c data, the compressible profile was divided into eight homogenous sublayers, including five in the highly organic silt loam layer and the remaining three equally dividing the silt loam layer. These sublayers will be used in the ILLICON analysis discussed later. Preconsolidation profile was interpreted by using cone tip stress values from a nearby CPT sounding, supplemented with the consolidation test results ("diamond" symbols) shown in Figure 2(c). The new embankment would have 7 to 10 ft of new fill, plus 5 ft of surcharge placed for nearly one year of waiting period. Therefore, the values of final effective vertical stress under maximum surcharge (P'_{vs}) at mid-depth of each sublayer can be estimated from $P'_{v0} + \Delta P'_{vs}$ using Boussinesq elastic stress distribution method for a long embankment. It can be seen that all, except the top sublayer, would have been normally consolidated after the maximum surcharge fill was placed. Each of the sublayers had a unique end-of-primary (EOP) e-log P'_v that was reconstructed by using Casagrande's method and consolidation data, all presented in Figure 3(a). As a result, it is expected that Sublayer Nos. 1 to 5 would accumulate the greatest settlements while Sublayer Nos. 6 to 8 would accumulate the least. For simplicity, each e-log P'_v curve was reconstructed by using single values of C_r and C_c although the EOP compression curve is generally non-linear.

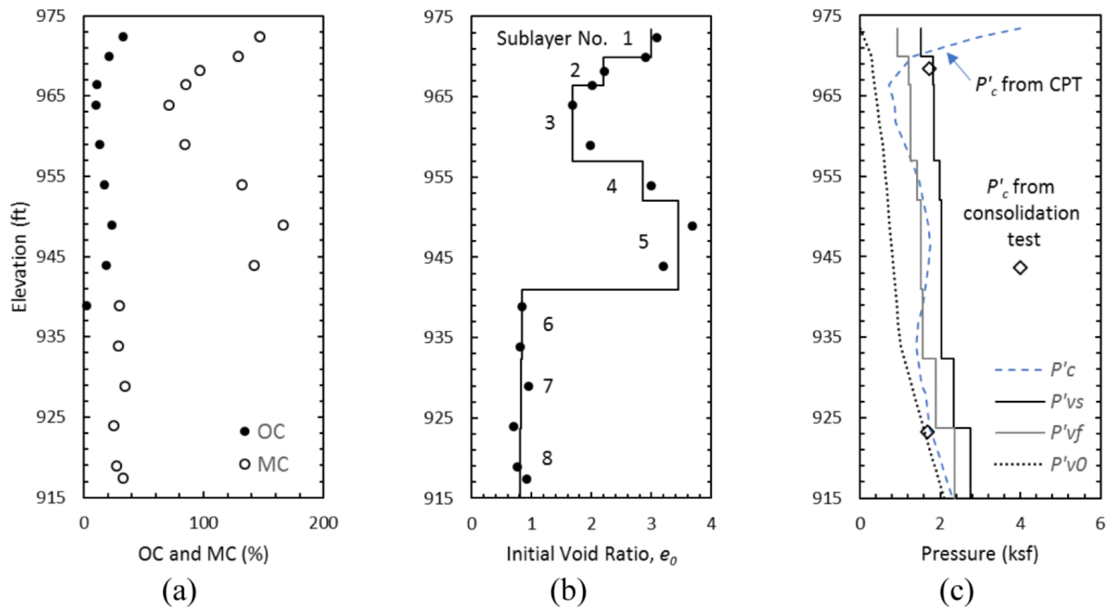

Figure 2. Vertical profiles for (a) Organic and moisture contents, (b) Initial void ratio, and (c) P'_{v0}, P'_c and P'_{vs}

Coefficient of permeability (k_v) and permeability change index (C_k)

When Terzaghi's theory of one-dimensional consolidation is used for computing time-settlement relationship, the coefficient of consolidation (c_v) is required. The values of c_v can be estimated from the time-deformation data, by the classical "curve-fitting methods" developed by Casagrande and Taylor or the inflection point method (Robinson 1997). It is important to recall that Terzaghi's theory is based on several major assumptions, including: small strain and one-dimensional strain, incompressible soil grains and pore fluid, homogenous and fully saturated soil, and constant compressibility and permeability during consolidation. The derivation of the closed-form solution leads to the following equation:

$$c_v = \frac{k_v(1+e)P_v^{'}}{0.434\gamma_w C_c} = \frac{k_v m_v}{\gamma_w} \quad (1)$$

where k_v = coefficient of permeability, P'_v = vertical effective stress, and m_v = constrained modulus. However, it is widely known that c_v is not constant, not to mention that k_v and m_v exhibit significant variation during consolidation process when void ratio is reduced. As a result, the use of c_v can produce erroneous results in a time-settlement analysis. Alternatively, permeability change index (C_k) can be used to better represent the reduction in coefficient of permeability during compression:

$$C_k = \frac{e_0 - e}{\log k - logk_0} \quad (2)$$

This relationship can also be integrated into the finite-strain hydrodynamic equation, such as the ILLICON approach used in this case study. In the past, empirical correlation between C_k and e_0 had been developed for clay deposits, such as a typical value of $C_k/e_0 = 0.5$ in soft clay (Tavenas et al. 1983). A low C_k indicates dramatic decrease in permeability when effective stress increases, which means that the dissipation rate of excess pore water pressure reduces over time. By using the available consolidation test data, it is interesting to find that empirical correlations $C_k/e_0 = 0.26$ within the highly organic silt loam layer come close to the published data for highly organic clays and peat (Mesri and Ajlouni 2007, Terzaghi et al. 1996), shown in Figure 3(c).

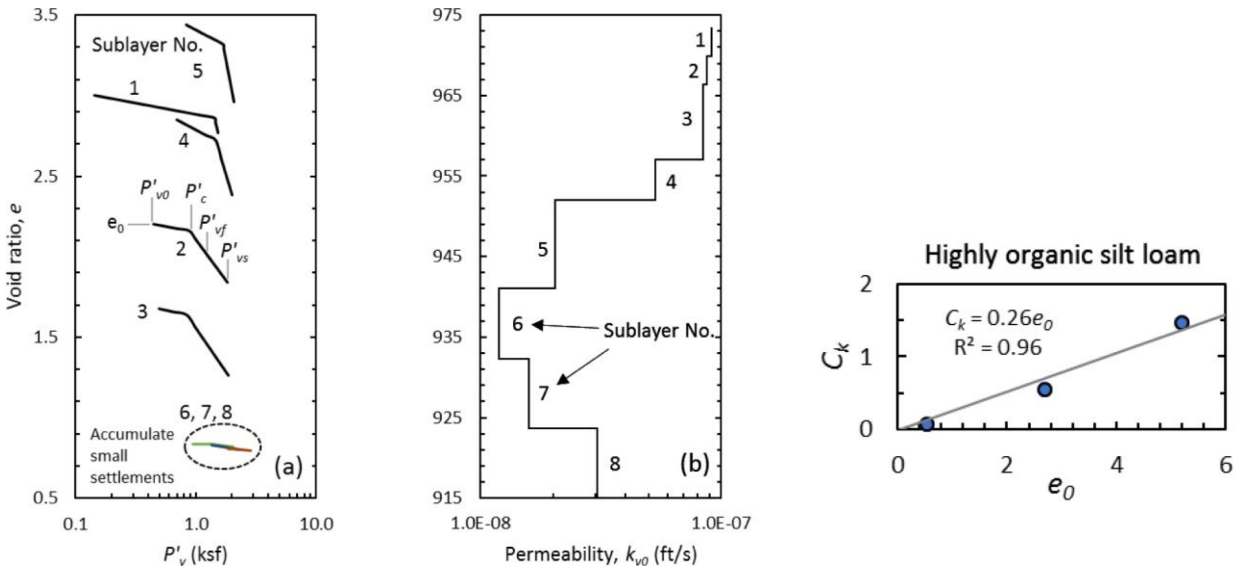

Figure 3. (a) Individual EOP *e*-log P'_v curve, (b) Initial permeability profile, and (c) C_k/e_0 relationship of the highly organic silt loam

Unfortunately, because there was no soil characteristic information (e.g. plasticity index or clay fraction) or direct measurement of permeability, selecting the preconstruction in-situ permeability required engineering judgment. The authors decided to estimate k_{v0} by applying Terzaghi's theory of consolidation and extrapolating to initial void ratio from the *e*-log k_v plots. As mentioned previously, Terzaghi's theory assumes a constant k_v which consequently may be unreasonably low, and thus only data within the compression range have been used to evaluate k_v.

PRIMARY SETTLEMENT BEHAVIOR

Time-settlement response

Primary settlement (S_p) response was back-analyzed based on the soil engineering properties and profiles as discussed above by using the ILLICON program. The vertical drains and soil radii were assumed to be 0.084 ft (a = 3.93 in and b = 0.12 in) and 0.63 ft, respectively, for a 6 ft triangular spacing pattern. The top and bottom drainage boundaries were assumed to represent a two-way drainage system. Since no k_h /k_v data was available, the anisotropy ratios were assumed to be 4.0 at the top three sublayers as surficial peat and 1.0 for the remaining sublayers. The computed settlements are shown in Figure 4(b), which agrees well with the measured settlements at the ground surface. Figure 4(b) also presents the computed settlements at the top of Sublayer Nos. 1 to 5 (Sublayer No. 1 being the surface settlement) and the estimated primary settlement based on a design c_v value of 0.18 ft^2/day (i.e. the method used during design to predict behavior). By comparing the c_v-estimated and measured settlements, it becomes evident that the time to achieve the end-of-primary consolidation is about 180 days by using the design c_v value, although field measured settlement continued to accumulate after 180 days. On the other hand, the computed settlement (red dash line) by using the ILLICON approach, which of course back-calculated based on the field data, shows how the interrelationships between void ratio, vertical effective stress, and permeability have been applied to model the consolidation process. These results indicate that Sublayers Nos. 2, 3 and 4, which were in compression range, accounted up to 70% of total settlement by Day 290.

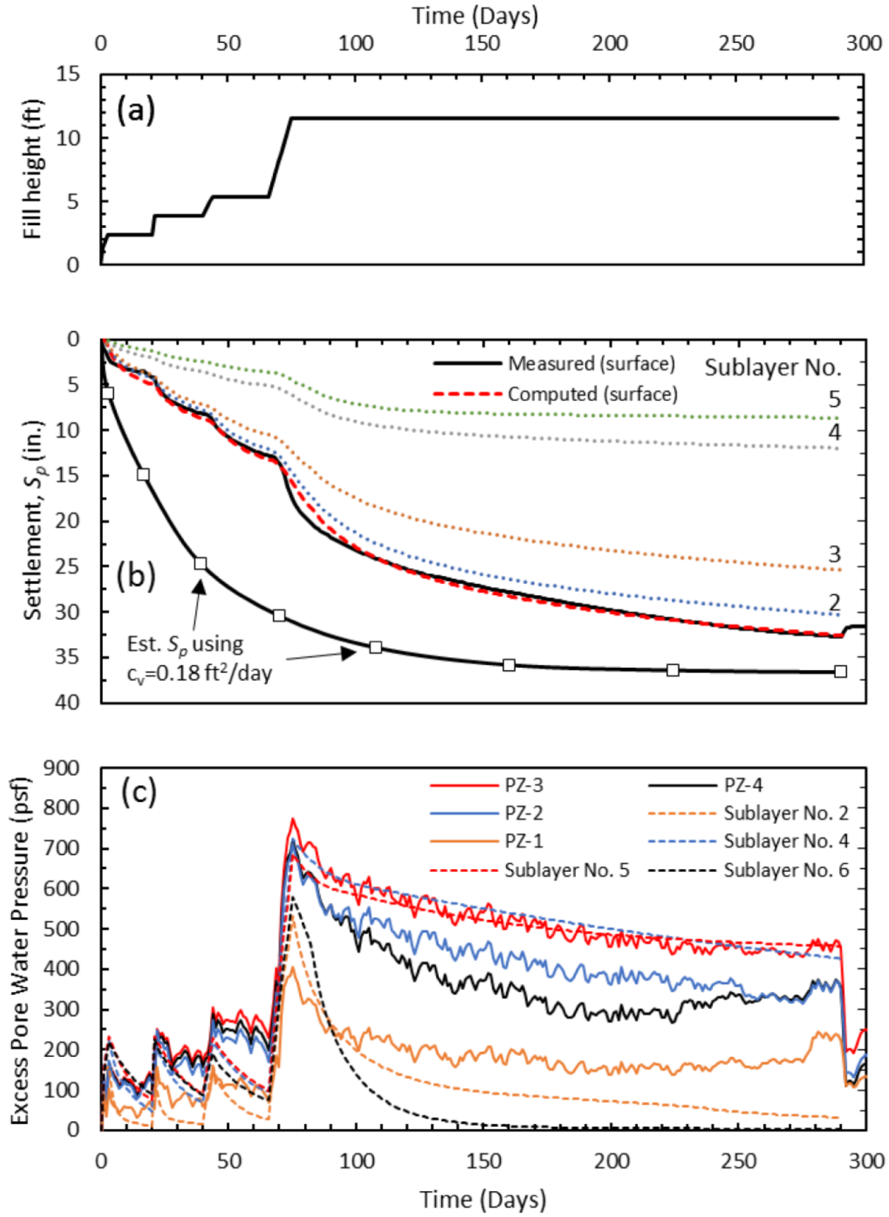

Figure 4. (a) Load history, (b) measured vs. computed settlement curves, and (c) measured vs. computed pore water response

Pore water pressure response

Figure 4(c) shows the measured and computed excess pore water pressure responses near the piezometer depths. For reference, PZ-1, PZ-2, PZ-3, and PZ-4 were installed at elevations 965, 955, 945 and 935 ft, respectively. Sublayer Nos. 2, 4, 5, and 6 represented the mid-depth elevations at 968.2, 954.5, 946.5, and 936.7 ft, respectively. By comparing the results, it becomes obvious that excess pore water pressure, especially at PZ-2 (cf. Sublayer No. 4), PZ-3 (cf. Sublayer No. 5), and PZ-4 (cf. Sublayer No. 6), dissipated at a slower rate after the last stage of fill was placed on about Day 70. This confirms that soils within this layer had relatively low C_k, or in other words, the permeability reduced significantly when compressed. Nevertheless, it appears that permeability in Sublayer No. 6 could be overestimated, resulting in lower predicted excess pore water pressure than measured. Another possible explanation is if PZ-4 was installed in the highly organic silt loam instead of the modeled silt loam layer. Because the borings drilled for piezometer installation were not sampled, it is unknown whether this may have been the case.

POST-SURCHARGE SECONDARY SETTLEMENT BEHAVIOR

For an embankment (founded on soft ground) that experienced surcharge loading, the removal of surcharge would lead to rebound, followed by post-surcharge secondary settlement. This response has been described in literature and past studies (e.g. Terzaghi et al. 1996, Mesri et al. 2001). In general, the removal of surcharge causes a rebound, including primary rebound up to t_{pr} and secondary rebound that levels off at t_l, followed by secondary compression which is described by post-surcharge secondary compression index, C'_α and its secant form, C''_α due to non-linearity of the precedent. The settlement occurring after removal of the surcharge can be estimated by using the equation below:

$$S = \frac{\frac{C''_\alpha}{C_\alpha} \times \frac{C_\alpha}{C_c} \times C_c}{1+e_0} H_0 \log\left(\frac{t}{t_l}\right) \tag{3}$$

where C_c = compression index, C_α = secondary compression index without surcharging = $\Delta e/\Delta \log t$, e_0 = initial void ratio, H_0 = initial compressible layer thickness, and t = time of interest. It is important to note that for practical estimation of secondary settlement, the above equation only considers secant C''_α because C'_α is not constant over time (see next figure); however, laboratory observations of EOP e-log P'_v suggested that C'_α starts at a small value, gradually increases, and eventually decreases with time or becomes constant.

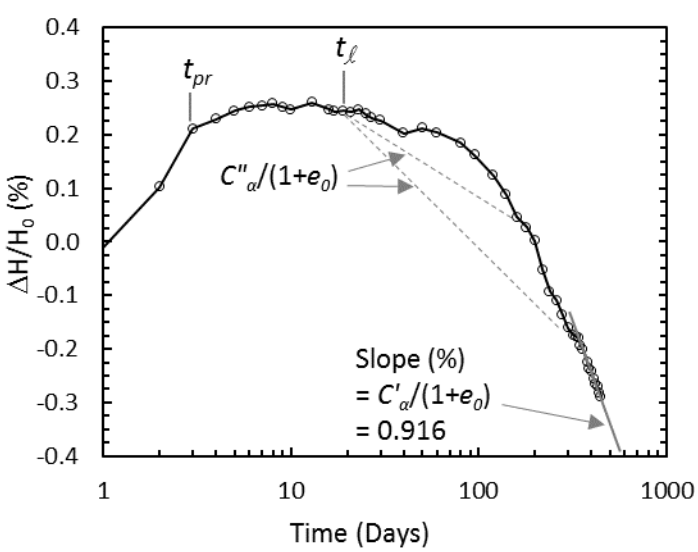

Figure 5. Post-surcharge secondary settlement measured at the site (time *t* =1 corresponds to the day surcharge was removed).

In this case, the field measurement of secondary compression data for 460 days after the removal of surcharge is plotted in Figure 5 above. The measured settlement after the removal of surcharge is ΔH, and $\Delta H/H_0$ is conveniently used for arriving at $C'_\alpha/(1+e_0)$ values. Both C''_α and C'_α were not directly evaluated through laboratory tests, but field data suggests that the settlement has a downward slope of 0.0092 (or 0.92%) from Day 300 to Day 460 and is relatively constant or changing at a slow rate (unknown because monitoring was discontinued after Day 460). This slope from the plot can be related to C'_α by the following equation:

$$\frac{C'_\alpha}{1+e_0}=\frac{(\Delta H)/H_0}{\Delta \log t} \tag{4}$$

According to the C_α/C_c law of compressibility, for a given soil, C_α/C_c is a constant and independent of time, effective stress, and compression history. Therefore, the same C_α/C_c is applicable to recompression, compression, and even after surcharging. The effectiveness of the surcharge can be represented by a ratio of C'_α/C_α, which if less than one indicates successful precompression (i.e. effectively reducing C_α). Recall that C_α/C_c is 0.051, the ratio of C'_α/C_α thus ranges from 0.38 to 0.64 for the highly organic silty clay loam, by assuming the slope = $C'_\alpha/(1+e_0)$ obtained from Figure 5.

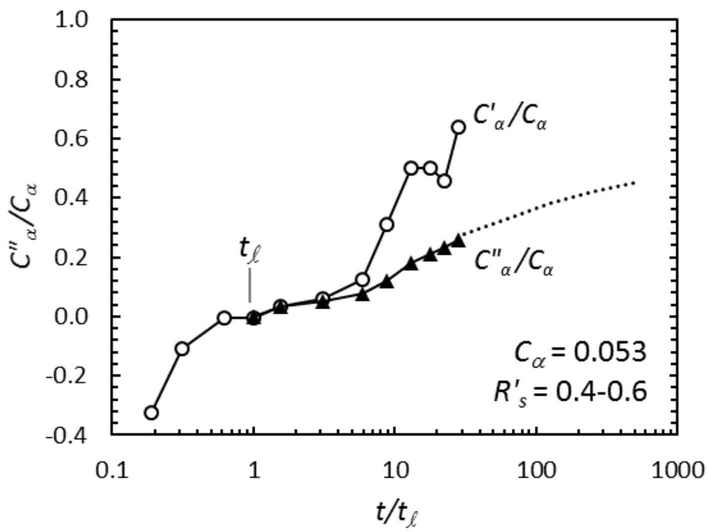

Figure 6. Post-surcharge secondary and secant secondary compression indices of highly organic silty clay loam in Nicollet, MN.

After surcharging, the stress states were "returned" to P'_{vf} which laid on the compression curve (see Figure 2(c) for P'_{vf} and P'_{vs}), especially for Sublayer Nos. 2, 3, and 4. Usually, C_c along the compression curve decreases slightly as P'_v increases; therefore, the value of C_α should also decrease slightly with time. For simplicity, however, a single value of C_α can be used to normalize the C'_α obtained from the field data. Using the same set of field data and C_α, a series of C'_α/C_α and C''_α/C_α points were computed and are presented in Figure 6 above. In this figure, C'_α/C_α started at -0.33 (negative indicates rebound), leveled off at about $t/t_l=1$, then trended upward (compression) to 0.64 at Day 460. After increasing for some time, C'_α/C_α is expected to decrease, but never become 1.0, because C_c continues to decrease as P'_v increases on the compression curve. In other words, values of C'_α at the future time can be reasonably predicted by using $C_\alpha/C_c = C'_\alpha/C_c = 0.051$ and values of C_c on the compression curve (Mesri 1986). Similarly, C''_α/C_α which was derived relative to t_l, continually increased to 0.26 at Day 460 and is expected to gradually (i.e. due to slowdown of C'_α / C_α) increase for an unknown amount of time until it approaches 1.0. This C''_α / C_α line of course is only valid for the effective surcharge ratio, $R'_s = (P'_{vs} / P'_{vf}) - 1 = 0.4$ to 0.6, which correspond to the mid-depth stress states of Sublayer Nos. 2, 3 and 4. The post-surcharge secondary settlement at a given t/t_l can thus be estimated from Eqn. (3). By using the data shown in Figure 5, the projected C''_α / C_α is represented by the dotted line in Figure 6 — C''_α / C_α continues to slowly increase to 0.45. Using this value, the estimated secondary settlement from t_l until 25-years following surcharge removal is projected to be 6.7 inches. Hence, the estimated total secondary settlement minus rebound of 0.9 inch is 5.8 inches. One could question if the slope of $C'_\alpha/(1+e_0) = 0.92\%$ (in Figure 5) can be used to estimate the future settlement. Accordingly, the projected settlement after 25 years would be about 5 inches; total secondary settlement would then be 5 inches – 0.9 inches (rebound) = 4.1 inches (less than the 5.8 inches prediction). The authors, however, would like to emphasize that since C'_α is expected to decrease over time (even though at a slow rate), projecting future settlement by using the seemingly constant C'_α is likely to underestimate the settlement.

CONCLUDING REMARKS

This paper consists of three parts: (i) Interpretation of laboratory and subsurface investigation data, (ii) Back-analysis of primary settlement response by comparing with field data, and (iii) Use of limited field and laboratory data to estimate future post-surcharge secondary settlement. Although several assumptions were made for all parts, the authors have applied soil mechanics, or, more importantly, highly organic soil's engineering behavior, and empirical correlations to arrive at reasonable conformation and agreement on model computations in parts (i) and (ii). Permeability change index (C_k) is especially useful in representing the compressibility and permeability relationship of highly organic soils. More details about the project background information, project challenges, ground improvement decision process, and geotechnical instrumentation can be found in Lamb et al. (2018). In part (iii), an approach (i.e. Mesri et al. 2001) was introduced for explaining post-surcharge rebound and secondary settlement behavior that was measured using modern geotechnical instrumentation. Based on the observation of field data and anticipated actual field conditions, indices such as C'_α, C''_α, and C_α / C_c have been used to understand the development of time-deformation relationship and to thereby project the future settlement.

REFERENCES

Lamb, R.A., Chow, L. C. and Bentler, J. G. (2018) "US Highway 14 embankment over soft soils – success with ground improvement and modern instrumentation." *66th Annual Geotechnical Engineering Conference*, University of Minnesota, St. Paul, MN, 117-126.

Mesri, G. and Choi, Y. K. (1985). "Settlement analysis of embankments on soft clays." *ASCE Journal of Geotechnical Division*, 111(4), 441-464.

Mesri, G. (1986). "Discussion of 'Post-construction settlement of an expressway built on peat by precompression.'" *Canadian Geotechnical Journal*, 23(3), 403-407.

Mesri, G., Ajlouni, M. A., Feng, T. W. and Lo, D. O. K. (2001). "Surcharging of soft ground to reduce secondary settlement." *3rd International Conference on Soft Soil Engineering*, Hong Kong, 55-66.

Mesri, G. and Ajlouni, M. A. (2007). "Engineering properties of fibrous peats." *ASCE Journal of Geotechnical and Geoenvironmental Engineering*, 133, 850-866.

Robertson, P. K., Campanella, R. K., Gillespie, D. and Greig, J. (1986). "Use of piezometer cone data." *In-Situ '86: Use of In-Situ Testing in Geotechnical Engineering*, Geotechnical Special Publication 6, Reston, VA, 1263-1280.

Robinson, R.G. (1997). "Consolidation analysis by an inflection point method." *Géotechnique*, 47(1), 199-200.

Tavenas, F., Jean, P., Leblond, P. and Leroueil, S. (1983). "The permeability of natural soft clays. Part II: permeability characteristics." *Canadian Geotechnical Journal*, 20, 645-660.

Terzaghi, K., Peck., R. B. and Mesri, G. (1996). *Soil Mechanics in Engineering Practices*. 3rd Edition. New York: John Wiley and Sons.